Bull. Mater. Sci. (2018) 41:161
https://doi.org/10.1007/s12034-018-1675-2

Microwave-hydrothermal synthesis of mesoporous γ-Al_2O_3 and its impregnation with AgNPs for excellent catalytic oxidation of CO

SUKANYA KUNDU and MILAN KANTI NASKAR*
Sol–Gel Division, CSIR-Central Glass and Ceramic Research Institute, Kolkata 700 032, India
*Author for correspondence (milan@cgcri.res.in)

MS received 2 January 2018; accepted 7 March 2018

Abstract. Mesoporous γ-alumina was synthesized by the microwave-hydrothermal process with a shorter duration time at 150°C/2 h followed by calcination at 550°C/1 h. Ag nanoparticles (AgNPs) were impregnated into γ-alumina under a reducing atmosphere at 450°C. The synthesized product was characterized by X-ray diffraction (XRD), thermogravimetric (TG)/differential thermal analysis (DTA), X-ray photoelectron spectroscopy (XPS), N_2 adsorption–desorption study, field-emission scanning electron microscopy (FESEM) and transmission electron microscopy (TEM). The BET surface area values of γ-alumina and Ag-impregnated γ-alumina were found to be 258 and 230 $m^2\ g^{-1}$, respectively. FESEM images showed the formation of grain-like particles of 50–70 nm in size with a flake-like microstructure. The XRD, XPS and TEM studies confirmed the presence of Ag in the synthesized product. Catalytic properties of the product for CO oxidation was studied with the T_{50} (50% conversion) and T_{100} (100% conversion) values of 118 and 135°C, respectively; the enhanced values were compared with the literature reported values.

Keywords. Microwave hydrothermal; microstructure; mesoporous Al_2O_3; CO oxidation.

1. Introduction

Mesoporous γ-Al_2O_3 is used as a catalyst, catalyst support, membrane, adsorbent and high-performance ceramic due to its properties like four-fold co-ordination, high surface area, thermal stability etc. The synthesis of mesoporous γ-Al_2O_3 has been reported using different methods, like sol–gel [1], evaporation-induced self-assembly (EISA) [2,3], hard-template route [4], flame pyrolysis [5], control precipitation [6], hydrothermal [7], combustion synthesis [8] etc. Recently, microwave heating is a widely used technique for material synthesis due to its several advantages like rapid volumetric heating, dramatic increase in reaction rates, direct interaction of microwave energy with the reaction system, short reaction time and reduced energy consumption as opposed to the conventional heating process [9,10]. Synthesis of mesoporous alumina by the microwave-assisted hydrothermal method has rarely been reported.

Carbon monoxide (CO) is a common by-product produced from incomplete combustion reactions, and it is a harmful air pollutant in the urban areas. It is a very toxic gas for humans and animals as it has high affinity with haemoglobin [11], causing detrimental effects on the nervous system and cardiac function [12,13] with its concentration greater than 100 ppm. Catalytic oxidation is an efficient method for complete removal of CO, and it finds variety of practical applications, such as automobile exhaust purifiers, CO gas masks, CO sensors, CO removal in heavy industries etc. [14]. Expensive noble metals such as Pt, Au, Pd etc. are commonly used as catalysts for catalytic oxidation of CO. Li *et al* [15] used mesoporous alumina-supported noble metal nanoparticles because of their catalytic activities for CO oxidation. Due to the cost factor, low cost transition-metal-impregnated supported materials have been used for the catalytic oxidation of CO [16,17]. Ag is a relatively low-cost noble metal compared with Pt, Pd and Au. Different Ag-supported oxides fabricated through various methods show catalytic performance towards CO oxidation [18,19]. Krisztina *et al* [20] synthesized Ag/TiO_2 catalysts by a co-precipitation method for CO oxidation. Yu *et al* [21] reported that the catalytic performance of SiO_2-supported silver nanoparticles towards CO oxidation at ambient temperature is quite low due to the presence of agglomerated particles and the single phase of the support materials.

In this study, mesoporous γ-Al_2O_3 was synthesized by calcination of boehmite particles prepared *via* the microwave-assisted hydrothermal process with a shorter duration time at 150°C/2 h followed by wet-impregnation of Ag nanoparticles (AgNPs) into the synthesized γ-Al_2O_3 under a reducing atmosphere at 450°C. The catalytic performances of Ag/Al_2O_3 for the oxidation of CO were investigated in this work. This work is significant in two aspects: firstly, synthesis of mesoporous γ-Al_2O_3 *via* the microwave-assisted hydrothermal process at 150°C for a shorter duration time (2 h) followed by calcination at 550°C, and secondly, the enhanced catalytic efficiency of Ag/Al_2O_3 for CO oxidation compared with that from the literature reports.

Published online: 05 December 2018

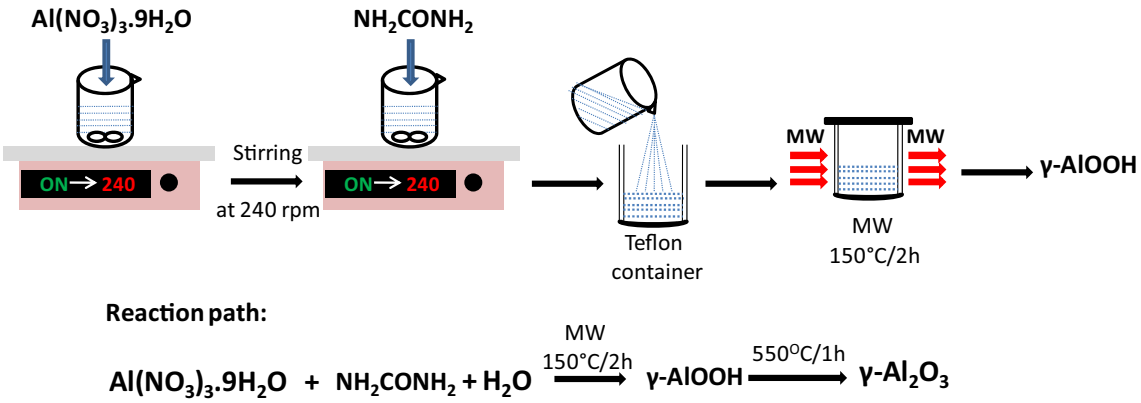

Scheme 1. Synthesis steps for the formation of γ-alumina *via* the microwave-assisted hydrothermal process.

2. Materials and methods

2.1 *Material preparation*

In a typical experiment, 0.25 mmol $Al(NO_3)_3{\cdot}9H_2O$ (G.R. Merck, India, purity >99%) was dissolved in 200 ml of DI water under stirring for 10 min at room temperature. Five mmol urea (99%, Sigma-Aldrich, USA) was added into the above solution. The mixture solution was kept under stirring condition for 30 min followed by a microwave reaction (Microsynth T660, Milestone, Italy) at 150°C for 2 h. Then the obtained precipitate was centrifuged and washed—three to four times the neutral pH. The wet sample was dried overnight at 70°C in an air oven. The dried product was heated at 550°C/1 h under a normal air atmosphere to obtain γ-alumina. The sample was designated as A20U. The synthesis procedure for the formation of γ-alumina is shown in scheme 1.

For impregnation of AgNPs into the synthesized γ-Al_2O_3, 60 mg of γ-Al_2O_3 was added into 15 ml aqueous solution of 5 mol% $AgNO_3$ with respect to γ-Al_2O_3. The mixture solution was kept under stirring condition for 5 h. The above solution was dried in an air oven at 60°C. The dried powder was then calcined at 450°C for 2 h at a heating rate of 2°C min^{-1} under a reducing atmosphere of He–5% H_2 gas maintaining a flow rate of 40 ml min^{-1}. The calcined product impregnated with Ag into γ-Al_2O_3 was designated as A20U-Ag.

2.2 *Characterization*

The product was characterized by X-ray diffraction (XRD) (Philips X'Pert Pro PW 3050/60, Ni-filtered Cu-Kα radiation, λ = 0.15418 nm), differential thermal analysis/thermogravimetric (DTA/TG) (Netzsch, Germany), X-ray photoelectron spectroscopy (XPS) (ULVAC-PHI, USA), nitrogen adsorption–desorption (Quantachrome (ASIQ MP), field-emission scanning electron microscopy (FESEM) (Zeiss, Supra^{TM} 35VP, Oberkochen, Germany) and transmission electron microscopy (TEM) (Tecnai G2 30ST, FEI).

2.3 *Catalytic test*

A continuous flow fixed-bed glass tubular reactor (i.d.: 4 mm) was used to carry out the catalytic test for the CO oxidation. In this experiment, 50 mg of A20U-Ag was used. Before experiment, the system was calibrated by using a standard calibration gas (1, 2 and 3 vol% CO). Then, a standard reaction gas mixture (1 vol% CO, 20 vol% O_2 and rest N_2) was introduced at the 40 ml min^{-1} flow rate into the bed. The converted output gas was measured by using a GC (Varian CP3800). The percentage CO conversion was calculated from the area under the peak [22]:

$$\%\ \text{Conversion} = \text{area under } CO_2 \text{ peak}/(\text{area under CO peak} + \text{area under } CO_2 \text{ peak}). \quad (1)$$

The conversion of CO to CO_2 was measured at different temperatures. The conversion rate of CO per unit surface area per second was obtained from the following equation:

$$\text{Conversion rate [mol s}^{-1}\text{ m}^{-2}] = C_{CO} \times (X_{CO}/100)/(0.05 \times \text{SA}) \quad (2)$$

where C_{CO} is the number of moles of CO passed through the catalyst per second, X_{CO} is the percentage of CO conversion and the factor [0.05 × SA] represents the specific surface area for 50 mg of catalyst and SA is the BET surface area.

3. Results and discussion

3.1 *Characterization*

Figure 1 presents the XRD patterns of (a) the as-prepared γ-AlOOH, (b) A20U (γ-Al_2O_3) and (c) A20U-Ag (Ag-impregnated γ-Al_2O_3). The orthorhombic boehmite phase (JCPDS file no. 03-0065) was found in the as-prepared uncalcined sample obtained by the microwave-assisted hydrothermal process, which is transformed to the cubic γ-alumina

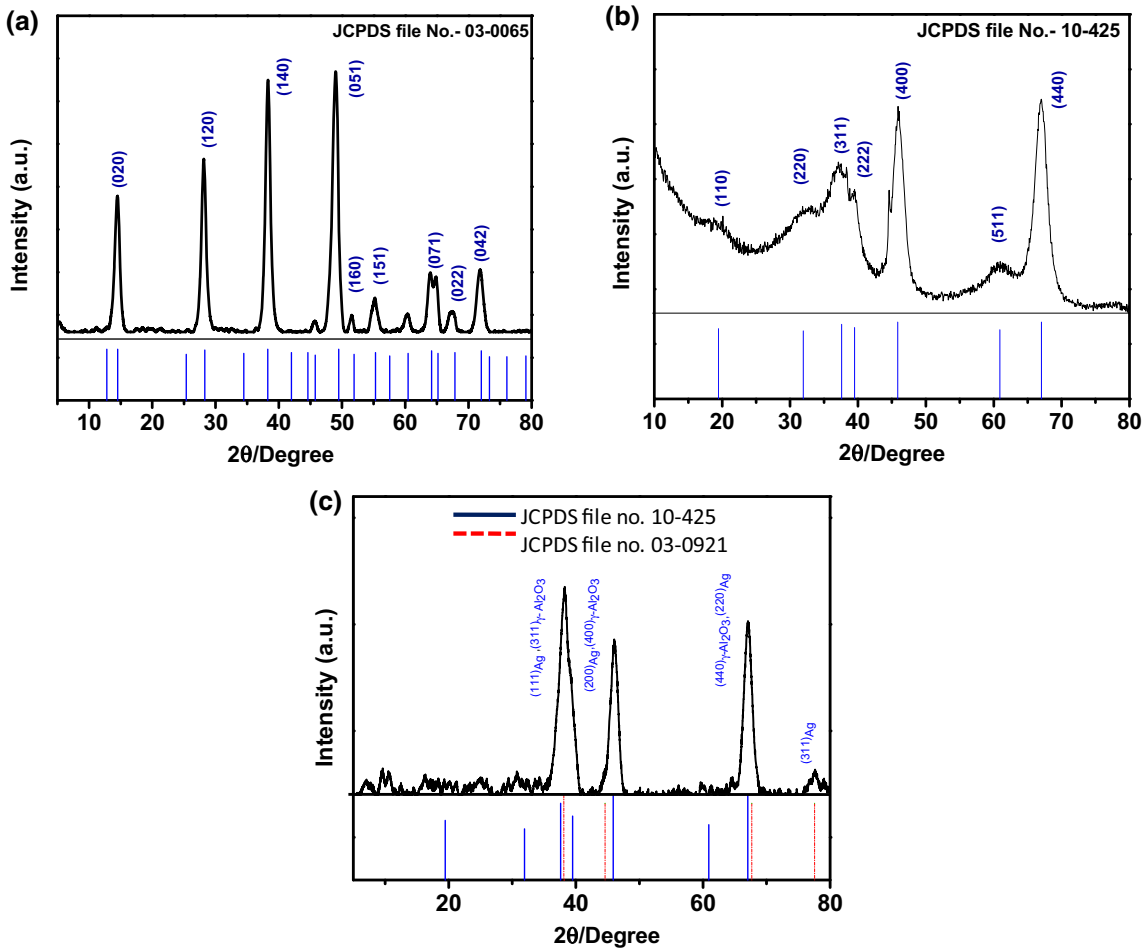

Figure 1. XRD patterns of (**a**) the as-prepared γ-AlOOH, (**b**) A20U (γ-Al_2O_3) and (**c**) A20U-Ag (AgNP-impregnated γ-Al_2O_3).

phase (JCPDS file no. 10-425) after calcination at 550°C/1 h (figure 1b). Interestingly, in the sample A20U-Ag, in addition to the crystallization of γ-alumina, the metallic Ag (JCPDS no. 03-0921) was also present. The crystal planes of Ag are (111), (200), (220) and (311) confirming the impregnation of Ag in γ-Al_2O_3.

In the DTA curve (figure 2), the sharp endothermic peaks are observed at 96 and 458°C accompanying by one exothermic peak at 260°C. The first endothermic peak at 96°C is attributed to the removal of surface-absorbed water while the second endothermic peak at 458°C is ascribed to the transformation of boehmite (γ-AlOOH) to γ-Al_2O_3. The exothermic peak at 260°C indicates the decomposition of nitrates from the precursor $Al(NO_3)_3$. The TGA curve (figure 2) shows that the maximum mass loss of 23.7% occurred up to 550°C. It corroborated with the removal of H_2O, decomposition of nitrates/other volatiles and conversion of γ-AlOOH to the γ-Al_2O_3 phase.

Figure 3a reveals the XPS data of the A20U-Ag sample in the full spectrum indicating the presence of Ag 3d, Al (2s, 2p) and O (1s) spectra. The high-resolution XPS curve (figure 3b)

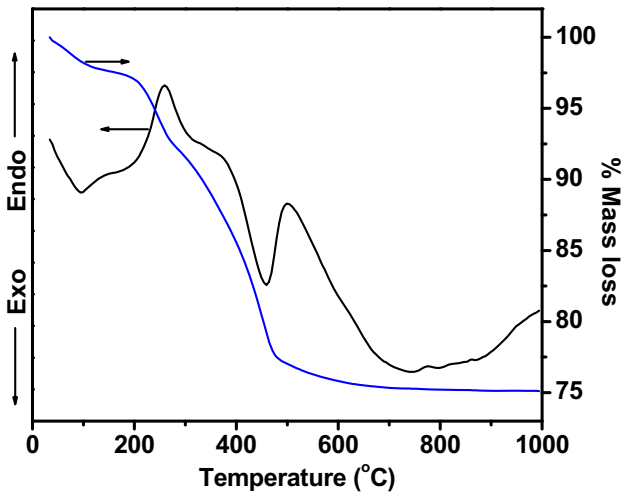

Figure 2. DTA and TG plots of A20U (uncalcined) before heat treatment.

of the Ag 3d region reveals the binding energies of Ag $3d_{5/2}$ and Ag $3d_{3/2}$ as 367.63 and 373.61 eV, respectively. The

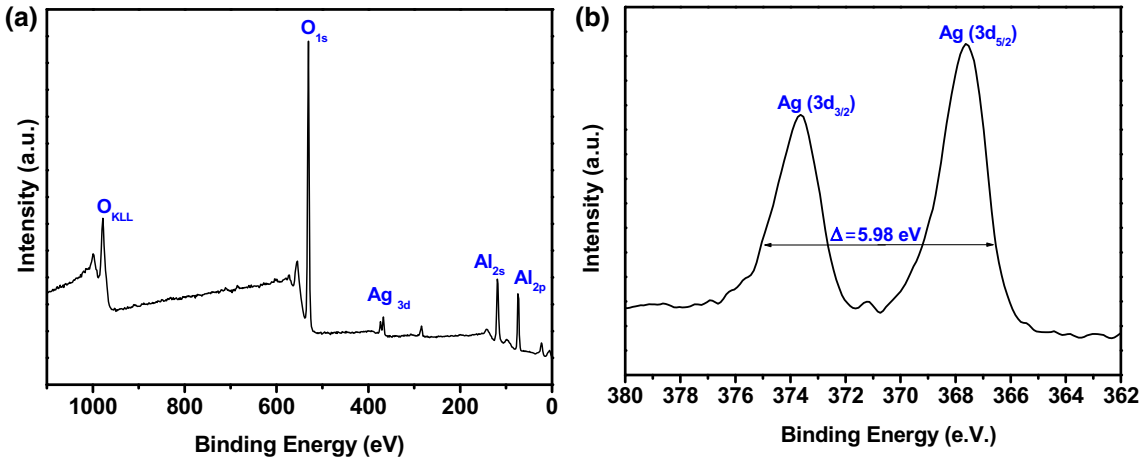

Figure 3. XPS of (**a**) survey spectra of A20U-Ag and (**b**) high-resolution spectra of Ag.

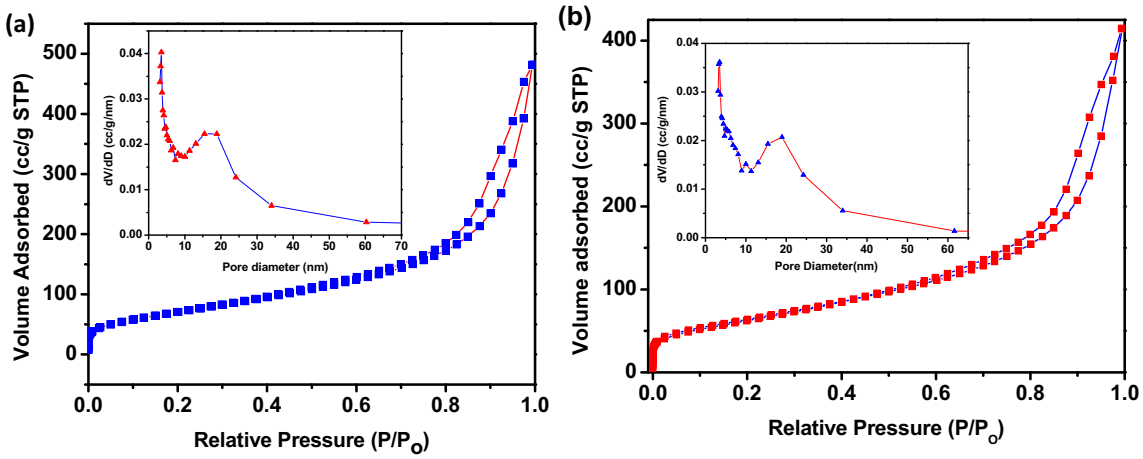

Figure 4. Nitrogen adsorption–desorption isotherms of (**a**) A20U (γ-Al_2O_3) and (**b**) A20U-Ag. Insets show the corresponding pore size distributions.

separation peak of Ag $3d_{5/2}$ and Ag $3d_{3/2}$ (5.98 eV) demonstrates the presence of Ag^0 (metallic Ag) in the A20U-Ag sample [23,24].

The nitrogen adsorption–desorption isotherms of γ-Al_2O_3 (A20U) is shown in figure 4a. It shows type-IV isotherms with a H3 hysteresis loop indicating interconnected slit-like mesopores. The pore size distribution of the same sample is shown in the inset of figure 4a. The BET surface area and pore volume of γ-Al_2O_3 (A20U) were found to be 258 $m^2\ g^{-1}$ and 0.7864 $cm^3\ g^{-1}$, respectively. To investigate the change of textural properties of γ-Al_2O_3 after impregnation of Ag, the nitrogen adsorption–desorption study of the A20U-Ag sample was conducted. Figure 4b shows the nitrogen adsorption–desorption isotherms of A20U-Ag, and the corresponding pore size distribution is depicted in the inset. However, no significant changes are found in the nature of isotherms and pore geometry between the pure γ-Al_2O_3 (A20U) and Ag-impregnated γ-Al_2O_3 (A20U-Ag). Interestingly, the values of the BET surface area (230 $m^2\ g^{-1}$) and pore volume (0.64 $cm^3\ g^{-1}$) decreased after impregnation of Ag into γ-Al_2O_3. However, the pore sizes of the samples before and after impregnation of Ag into γ-Al_2O_3 remained almost the same at around 3.5 nm.

Figure 5 shows the FESEM images of (a) the as-prepared boehmite, (b) γ-Al_2O_3 and (c, d) A20U-Ag. It is noted that a flake-like microstructure is formed in all the samples, indicating no morphological changes during the conversion of boehmite to γ-Al_2O_3, or even after impregnation of Ag into γ-Al_2O_3. Under the microwave-assisted hydrothermal process, flake-like particles are formed *via* the interaction of urea and Al^{3+} ions in aqueous medium (scheme 1). The highly magnified image of A20U-Ag (figure 5d) reveals that grain-like particles of 50–70 nm in sizes are assembled with a flake-like microstructure in a chain-like fashion. Under a microwave-assisted hydrothermal reaction boehmite nuclei are formed followed by the growth of

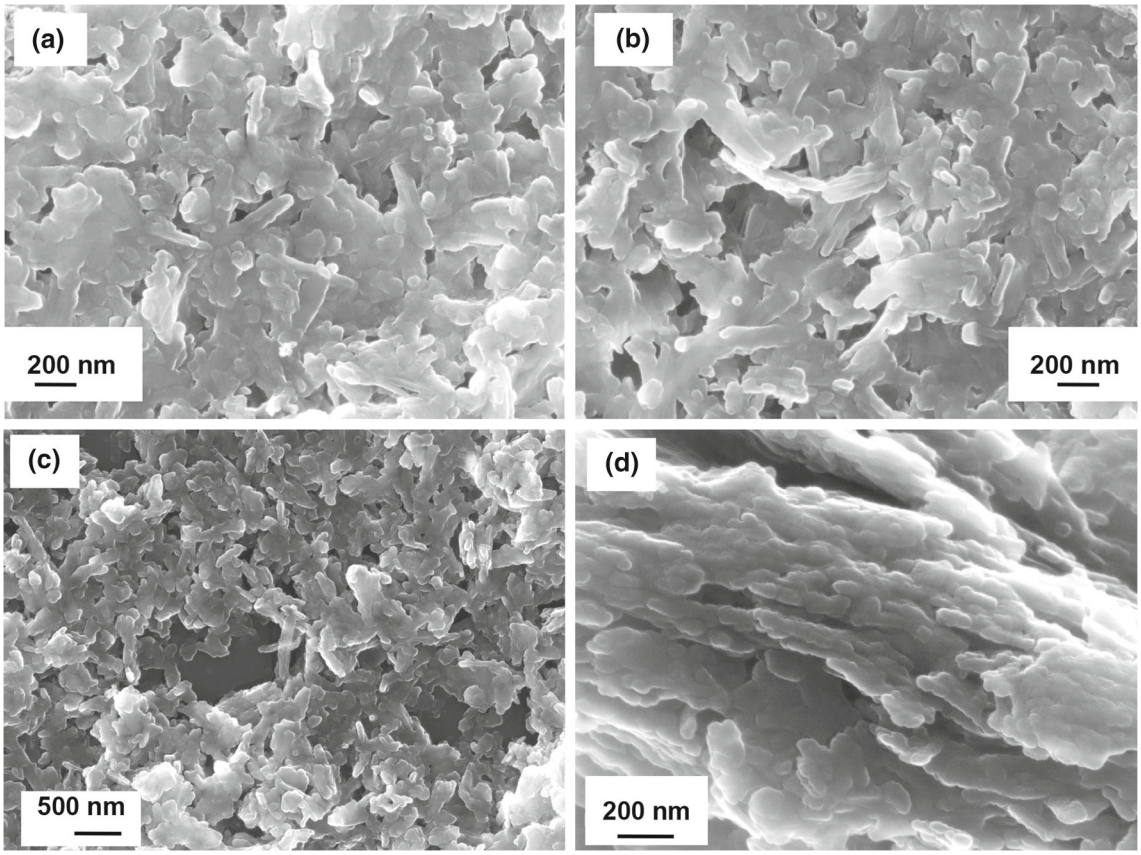

Figure 5. FESEM images of (**a**) the as-prepared boehmite sample, (**b**) γ-Al_2O_3 (A20U) and (**c**, **d**) A20U-Ag.

nanograin-like boehmite particles. These nanograin particles having the surface hydroxyl (–OH) groups interact with each other through hydrogen bonding towards the formation of flake-like particles. The decomposition of urea renders NH_3 and CO_2, which results in the formation of boehmite [25,26]. During calcination, the entrapped NH_3 and CO_2 and other decomposable products are evolved generating a porous structure.

The TEM images of A20U-Ag are shown in figure 6a and b indicating the porous microstructure of the sample. The particle size of AgNPs determined from the TEM images (counting at least 200 AgNPs) was found to be 5–10 nm while the same calculated from the Scherrer method was found to be 4.5 nm. The slightly bigger particle size calculated from the TEM images could be due to the agglomeration of AgNPs. The TEM images reveal that the AgNPs are dispersed in γ-Al_2O_3. The HR-TEM image of the A20U-Ag (figure 6c) shows the *d*-spacing of 0.22 nm due to the (111) plane of metallic Ag (Ag^0). The concentric diffraction rings corresponding to the (111), (200) and (220) planes of Ag^0 are also confirmed by the selected area electron diffraction (SAED) patterns (inset of figure 6c). The energy dispersive X-ray spectroscopy (EDS) analysis shows the presence of 1.27 atomic% of Ag in A20U-Ag (figure 6d).

3.2 *Catalytic performance*

The change in the catalytic conversion of CO to CO_2 with temperature of Ag-impregnated mesoporous γ-Al_2O_3 (A20U-Ag) is shown in figure 7a, and the inset shows the bar chart of percentage oxidation of CO at different temperatures. It is noted that the 50% conversion (T_{50}) of CO occurred at around 118°C, and 100% conversion (T_{100}) took place at 135°C. The present result for catalytic oxidation of CO was compared with the reported results (table 1) [12,19,27]. From the Arrhenius plots [ln(conversion rate) *vs.* $1/T$], it is clear that the efficiency of catalyst increased with temperature (figure 7b). This may be due to the synergetic effect between the metal and the support as well as the additional heat treatment under an O_2 ambience at high temperatures. Exposure to O_2 at high temperatures enhances the catalytic activity of the supported catalysts due to the formation of subsurface oxygen [28]. The better catalytic performance of Ag-impregnated alumina (A20U-Ag) compared with that of the previously reported literature is due to its higher surface area (table 1) providing more active catalytic sites. It has been reported that metal–support interaction could play an important role in catalytic oxidation of CO [29]. CO adsorption takes place on metallic sites; hence, the removal efficiency of CO on metallic sites is

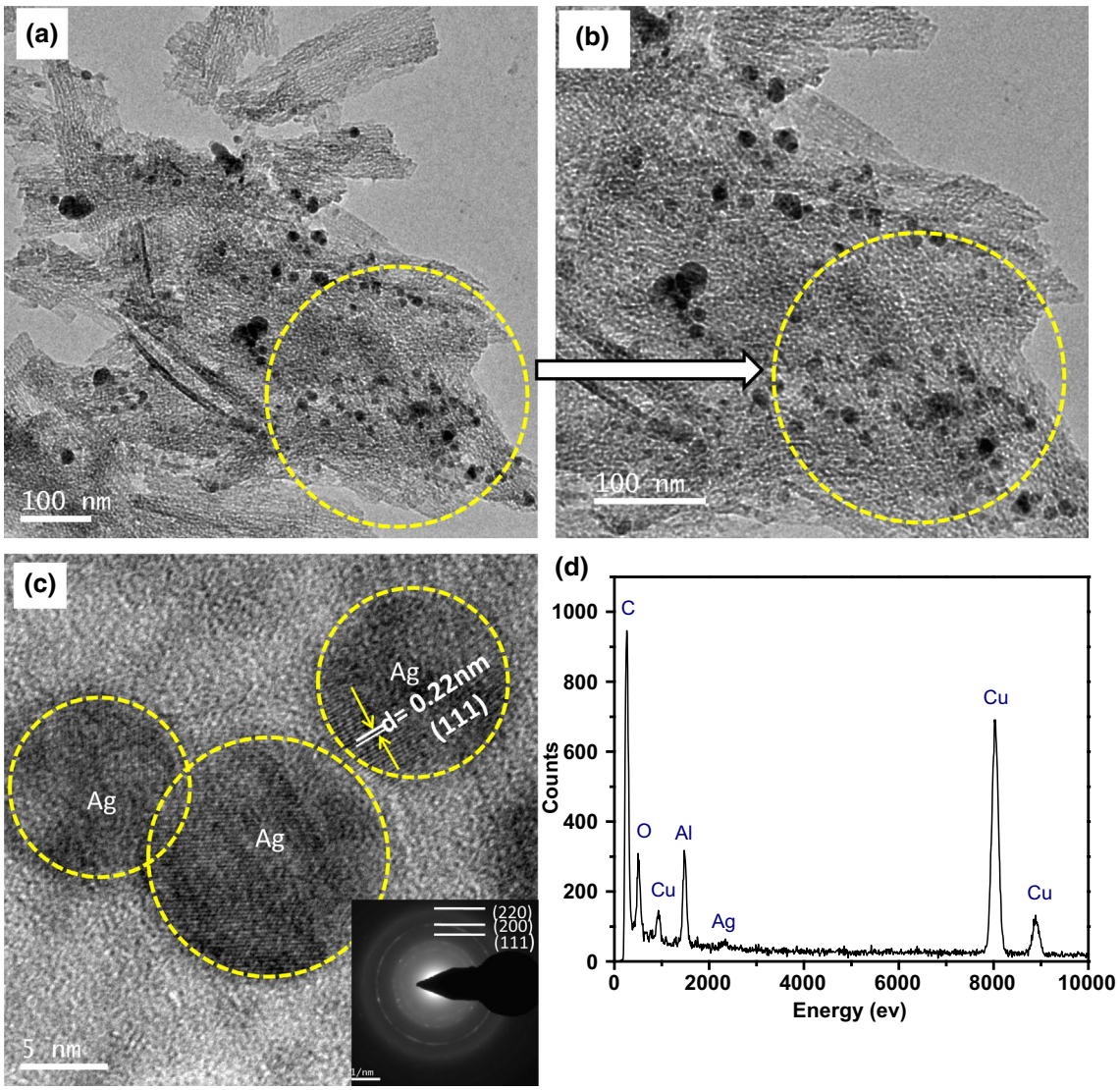

Figure 6. (**a**, **b**) TEM images, (**c**) HR-TEM (SAED patterns are shown in the inset) and (**d**) EDS of A20U-Ag.

easier in the catalyst with lower metal–support interaction. As the stability of metallic Ag is higher under normal conditions [30], the interaction of metallic Ag with the γ-Al_2O_3 support is lower in A20U-Ag. It is reported that the catalytic oxidation of CO is influenced by the oxygen adsorption ability and storage of the catalyst [31,32]. In the present case, the support material (porous alumina in the absence of AgNPs) and the blank glass tube with packing material could not show any catalytic efficiency for the oxidation of CO due to their lower oxygen adsorption ability and storage.

To understand the catalytic mechanism, it is to be noted that catalytic activity depends on CO adsorption onto the catalytic sites as well as desorption as CO_2 molecules. The adsorption of CO and O_2 on the metal surface is competitive. As a result, when CO is adsorbed on the metal site, it is difficult to adsorb O_2 molecules. In contrast, when the O_2 molecule is adsorbed first, the CO molecule can always find adsorption sites on the metal [33]. CO coverage on the metal surface is high due to its high mobility and high sticking coefficient. Adsorption of O_2 on the metal surface may occur in two steps:

$$O_2 + M_{(surf)} \rightarrow O_2 - M_{(surf)} \text{ (slow)} \quad (3)$$

$$O_2 - M_{(surf)} + M_{(surf)} \rightarrow 2O - M_{(surf)} \text{ (fast).} \quad (4)$$

In the first step, the O_2 adsorption process is very slow, but after adsorption, it is dissociated very quickly due to the low sticking coefficient of O_2 on the metal surface [34]. It is reported that heat of dissociative chemisorptions of O_2 is lower for metallic Ag [35]. For this reason, the catalytic efficiency of γ-Al_2O_3-supported Ag (A20U-Ag) shows better performance. It is inferred that catalytic efficiency depends not only on the surface area of the support but

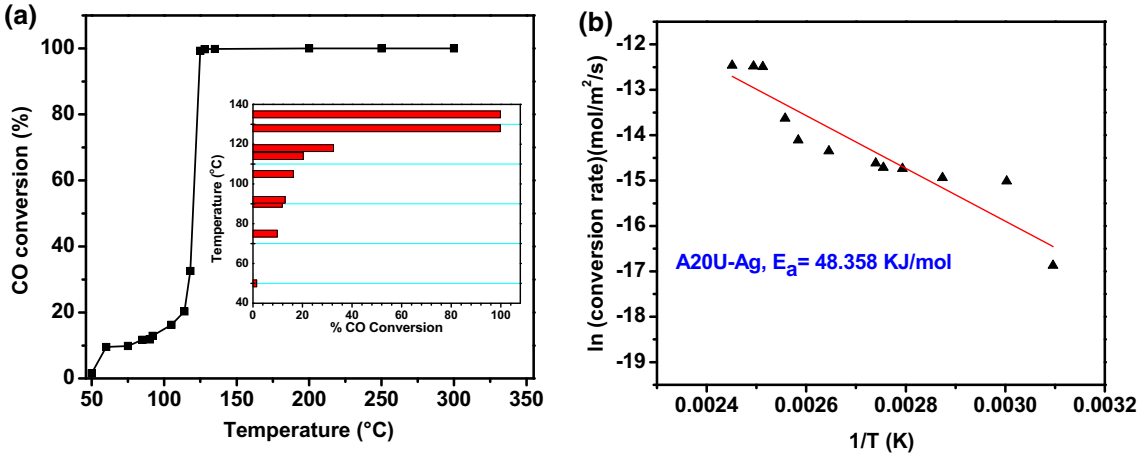

Figure 7. (**a**) Percentage of CO conversion *vs*. temperature (inset shows the bar chart of percentage oxidation of CO at different temperatures) and (**b**) Arrhenius plot for oxidation of CO for the catalyst A20U-Ag (feed gas composition: 1% CO, 20% O_2 and rest N_2; flow rate of feed gas: 40 ml min^{-1}; weight of the catalyst: 50 mg).

Table 1. Comparative study of CO oxidation for different Ag-based catalysts.

Sample	% CO conversion	Temperature (°C)	BET surface area (m^2 g^{-1})	References
Unsupported nanoporous Ag	95	145	22.5	[12]
Ag/SBA-15(F) (5.16 wt%) nanocomposites	100	270	220	[19]
Ag/CeO_2 (5%)	99	266	—	[27]
PdAg/CeO_2 (5%)	94	174	—	[27]
A20U-Ag	100	135	230	Present work

also on the metal support interaction; heat of dissociative chemisorption of O_2 on the metal surface plays a significant role.

4. Conclusions

Mesoporous γ-Al_2O_3 was prepared by the microwave-assisted hydrothermal process at 150°C with a shorter duration time (2 h) followed by heat treatment at 550°C/1 h. AgNPs were incorporated into γ-Al_2O_3 by the wet impregnation process followed by calcination at 450°C under a reducing atmosphere. The crystallization of boehmite and γ-Al_2O_3 along with metallic Ag was confirmed by XRD. In XPS study, the separation peak of Ag $3d_{5/2}$ and Ag $3d_{3/2}$ at 5.98 eV demonstrates the presence of metallic Ag in γ-Al_2O_3. The BET surface area of γ-Al_2O_3 decreased from 258 to 230 m^2 g^{-1} after Ag impregnation. Under the microwave-assisted hydrothermal process, flake-like particles are formed *via* the interaction of urea and Al^{3+} ions in aqueous medium, and no morphological changes occurred during the conversion of boehmite to γ-Al_2O_3, or even after impregnation of Ag into γ-Al_2O_3. AgNPs (5–10 nm) with 1.27 atomic% of Ag are dispersed as evidenced from the TEM study. The more catalytic efficiency for CO oxidation of the γ-Al_2O_3-supported Ag sample is due to its higher BET surface area, lower Ag–γ-Al_2O_3 interaction and lower heat of dissociative chemisorption of O_2 on the Ag surface. In general, the present method could be applicable for the synthesis of metal nanoparticle-impregnated ceramic oxides for the catalytic removal of toxic gases in the atmosphere.

Acknowledgements

The authors would like to thank the Director of CSIR-CGCRI for his kind permission to pursue this work. The author S.K., an AcSIR fellow, is grateful to CSIR, Government of India for her fellowship. The financial support from the Department of Science and Technology under the DST-SERB sponsored project, GAP 0616 (Grant No. SR/S3/ME/0035/2012), Government of India, is gratefully acknowledged.

References

[1] Tan H, Ma X and Fu M 2013 *Bull. Mater. Sci.* **36** 153
[2] Yang P, Zhao D, Margolese D I, Chmelka B F and Stucky G D 1998 *Nature* **396** 152
[3] Ghosh S, Dey K P and Naskar M K 2013 *J. Am. Ceram. Soc.* **96** 28

[4] Liu Q, Wang A, Wang X and Zhang T 2006 *Chem. Mater.* **18** 5153
[5] Tok A I Y, Boey F Y C and Zhao X L 2006 *Mater. Process. Technol.* **178** 270
[6] Parida K M, Pradhan A C, Das J and Sahu N 2009 *Mater. Chem. Phys.* **113** 244
[7] Li Y, Peng C, Li L and Rao P 2014 *J. Am. Ceram. Soc.* **97** 35
[8] Edrissi M and Norouzbeigi R 2011 *J. Am. Ceram. Soc.* **94** 4052
[9] Sivadasan A K, Selvam I P and Potty S N 2010 *Bull. Mater. Sci.* **33** 737
[10] Sommer W J and Weck M 2007 *Langmuir* **23** 11991
[11] Jones R A, Strickland J A, Stunkard J A and Siegel J 1971 *Toxicol. Appl. Pharmacol.* **19** 46
[12] Kou T, Lib D, Zhanga C, Zhanga Z and Yanga H 2014 *J. Mol. Catal. A: Chem.* **382** 55
[13] Townsend C L and Maynard R I 2002 *Occup. Environ. Med.* **59** 708
[14] Paldey S, Gedevanishvili S, Zhang W and Rasouli F 2005 *Appl. Catal. B* **56** 241
[15] Li Z X, Shi F B, Li L L, Zhang T and Yan C H 2011 *Phys. Chem. Chem. Phys.* **13** 2488
[16] Pillai U R and Deevi S 2006 *Appl. Catal. B* **64** 146
[17] Bose P, Ghosh S, Basak S and Naskar M K 2016 *J. Asian Ceram. Soc.* **4** 1
[18] Chen J L, Li J, Li H J, Huang X M and Shen W J 2008 *Microporous Mesoporous Mater.* **116** 586
[19] Tian D, Yong G P, Dai Y, Yan X Y and Liu S M 2009 *Catal. Lett.* **130** 211
[20] Frey K, Iablokov V, Melaet G, Guczi L and Kruse N 2008 *Catal. Lett.* **124** 74
[21] Yu L B, Shi Y Y, Zhao Z, Yin H B, Wei Y C, Liu J *et al* 2011 *Catal. Commun.* **12** 616
[22] Chowdhury I H, Ghosh S, Basak S and Naskar M K 2017 *J. Phys. Chem. Solids* **104** 103
[23] Wagner C D, Riggs W M, Davis L E, Moulder J F and Muilen-berg G E 1979 In *Handbook of X-ray Photoelectron Spectroscopy* (eds) Muilen-berg G E (Eden Prairie, MN: Perkin Elmer Corporation)
[24] Chowdhury I H, Ghosh S and Naskar M K 2016 *Ceram. Int.* **42** 2488
[25] Mishra D, Annad S, Panda R K and Das R P 2002 *Mater. Lett.* **53** 133
[26] Naskar M K 2009 *J. Am. Ceram. Soc.* **92** 2392
[27] Abdalsayed V, Aljarash A, El-Shall M S, Othman Z A A and Alghamdi A H 2009 *Chem. Mater.* **21** 2825
[28] Zhang X D, Qu Z P, Li X Y, Wen M, Quan X, Ma D *et al* 2010 *Sep. Purif. Technol.* **72** 395
[29] Ji L, Lin J and Zeng H C 2000 *J. Phys. Chem. B* **104** 1783
[30] Rattan G and Kumar M 2014 *Chem. Chem. Technol.* **8** 249
[31] Grunwaldt J D, Kiener C, Wogerbauer C and Baiker A 1999 *J. Catal.* **181** 223
[32] Wang W H and Cao G Y 2006 *Chin. J. Chem.* **24** 817
[33] Kolodziejczyk M, Colen R E R, Berdau M, Delmon B and Block J H 1997 *Surf. Sci.* **375** 235
[34] Royer S and Duprez D 2011*ChemCatChem* **3** 24
[35] Bligaard T, Norskov J K, Dahl S, Matthiesen J, Christensen C H and Sehested J 2004 *J. Catal.* **224** 206